Inorg. Chem. **2008**, *47*, 8748−8756

Template Synthesis of Lanthanide (Pr, Nd, Gd) Coordination Polymers with 2-Hydroxynicotinic Acid Exhibiting Ferro-/Antiferromagnetic Interaction

Na Xu, Wei Shi, Dai-Zheng Liao,* Shi-Ping Yan, and Peng Cheng

Department of Chemistry, Nankai University, Tianjin 300071, P. R. China

Received April 6, 2008

Lanthanide coordination polymers were synthesized from Pr(III), Nd(III), and Gd(III) salts; 2-hydroxynicotinic acid (Hnica); and $MnSO_4 \cdot H_2O$ under hydrothermal conditions. In the absence of $(CH_3)_3CCOONa$, 1D polymers with an infinite Ln(III)−O−Ln(III) chain structure, $[Pr(Hnica)(H_2O)_2SO_4]_n$ (**1**), $[Nd(Hnica)(H_2O)_2SO_4]_n$ (**2**), and $[Gd(Hnica)(H_2O)_2SO_4]_n$ (**3**), were generated. When $(CH_3)_3CCOONa$ was added to the synthetic systems, 2D coordination polymers $\{[Pr_3(Hnica)_6(H_2O)_9]\cdot 3H_2O\cdot SO_4\cdot NO_3\}_n$ (**4**), $\{[Nd_3(Hnica)_6(H_2O)_9]\cdot 3H_2O\cdot SO_4\cdot NO_3\}_n$ (**5**), and $\{[Gd(Hnica)_2(H_2O)_2]ClO_4\cdot H_2O\}_n$ (**6**) were obtained. Complexes **4** and **5** both exhibit Kagomé lattice structure, while **6** displays a rhombic grid structure. All complexes were characterized by elemental analysis, IR spectra, UV−vis spectra, and X-ray single-crystal diffraction. The variable-temperature magnetic susceptibility studies reveal ferromagnetic interactions between gadolinium(III) ions in **3** and **6** and antiferromagnetic interactions in **1**, **2**, **4**, and **5**.

Introduction

Lanthanide coordination polymers have been studied extensively because of their fascinating high-dimensional structures and potential applications as magnetic materials, molecular sensors, luminescent materials, absorption materials, and so on.[1−3] In the meantime, controlling the structure of the lanthanide coordination polymers is currently a formidable task due to the high coordination number and flexible coordination environments of lanthanide ions in comparison to that of transition metal coordination polymers.[4] Selection of multidentate ligands as spacers to link multiple lanthanide ions as nodes under suitable reaction conditions has been proved as a powerful methodology, and some important progress has been obtained. Among recent results, pyridine-dicarboxylic derivatives have been widely used as organic linkers to construct lanthanide coordination polymers with intriguing structures and promising properties. For example, unusual 3d−4f heterometallic coordination polymers have been synthesized by our group.[5] We continued our work on the pyridine derivatives with both carboxylic and hydroxyl functional groups, such as 2-hydroxynicotinic acid (H_2nica) and 6-hydroxynicotinic acid. The molecular structure of 2-hydroxynicotinic acid is shown in Scheme 1. While H_2nica has been widely utilized for synthesizing transition metal ion complexes,[6] only three isomorphic 1D lanthanide complexes formulated as $[Ln(Hnica)_2(\mu$-

* Author to whom correspondence should be addressed. E-mail: liaodz@nankai.edu.cn.

(1) (a) Bünzli, J. C. G.; Choppin, G. R. *Lanthanide Probes in Life, Chemical and Earth Sciences*; Elsevier: New York, 1989. (b) Valeur, B. *Molecular Fluorescence: Principles and Applications*; Wiley-VCH: New York, 2001.

(2) (a) Reineke, T. M.; Eddaoudi, M.; Fehr, M.; Kelley, D.; Yaghi, O. M. *J. Am. Chem. Soc.* **1999**, *121*, 1651. (b) Reineke, T. M.; Eddaoudi, M.; O'Keefe, M.; Yaghi, O. M. *Angew. Chem., Int. Ed.* **1999**, *38*, 2590. (c) Pan, L.; Huang, X. Y.; Li, J.; Wu, Y. G.; Zheng, N. W. *Angew. Chem., Int. Ed.* **2000**, *39*, 527. (d) Pan, L.; Adams, K. M.; Hernandez, H. E.; Wang, X. T.; Zheng, C.; Hattori, Y.; Kaneko, K. *J. Am. Chem. Soc.* **2003**, *125*, 3062. (e) Ma, B. Q.; Zhang, D. S.; Gao, S.; Jin, T. Z.; Yan, C. H.; Xu, G. X. *Angew. Chem., Int. Ed.* **2000**, *39*, 3644. (f) Long, D. L.; Blake, A. J.; Champness, N. R.; Wilson, C.; Schröder, M. *Angew. Chem., Int. Ed.* **2001**, *40*, 2444. (g) Goodgame, D. M. L.; Grachvogel, D. A.; White, A. J. P.; Williams, D. J. *Inorg. Chem.* **2001**, *40*, 6180. (h) Dalgarno, S. J.; Raston, C. L. *Chem. Commun.* **2002**, 2216. (i) Gheorghe, R.; Andruh, M.; Müller, A.; Schmidtmann, M. *Inorg. Chem.* **2002**, *41*, 5314. (j) Vaidhyanathan, R.; Natarajan, S.; Rao, C. N. R. *Inorg. Chem.* **2002**, *41*, 4496. (k) Almeida Paz, F. A.; Klinowski, J. *Chem. Commun.* **2003**, 1484. (l) Ghosh, S. K.; Bharadwaj, P. K. *Inorg. Chem.* **2005**, *44*, 3156. (m) Gándara, F.; García-Cortés, A.; Cascales, C.; Gómez-Lor, B.; Gutiérrez-Puebla, E.; Iglesias, M.; Monge, A.; Snejko, N. *Inorg. Chem.* **2007**, *46*, 3475.

(3) (a) Benellim, C.; Gatteschi, D. *Chem. Rev.* **2002**, *102*, 2369. (b) Robin, A. Y.; Fromm, K. M. *Coord. Chem. Rev.* **2006**, *250*, 2127.

(4) (a) Koeller, S.; Bernardinelli, G.; Bocquet, B.; Piguet, C. *Chem.—Eur. J.* **2003**, *9*, 1062. (b) Kepert, D. *Inorganic Stereochemistry*; Springer: Berlin, 1982; Chapters 2 and 12. (c) Bünzli, J. C. G. *Basic and Applied Aspects of Rare Earths*; Editional Complutense: Madrid, 1997.

10.1021/ic800623v CCC: $40.75
Published on Web 08/23/2008

Scheme 1. The Molecular Structure of 2-Hydroxynicotinic Acid and Its Tautomer

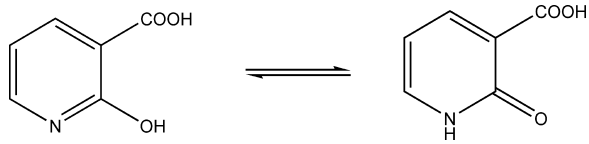

Hnica)(H_2O)]·nH_2O (Ln = Sm, Eu, Tb) and their crystal structures were reported, as far as we know.[7]

From the perspective of crystal engineering, self-assembly is a useful method to obtain prospective structure. Reaction conditions such as temperature, pressure, pH value, solvents, the ratio of reagents, and template agents play important roles for the self-assembly. In this field, inorganic−organic hybrid coordination polymers have attracted much attention because of their potential applications as molecular material.[8] Here, we report that applying a template agent, $(CH_3)_3CCOONa$, dramatically converted the 1D hybrid coordination polymers $[Pr(Hnica)(H_2O)_2SO_4]_n$ (**1**), $[Nd(Hnica)(H_2O)_2SO_4]_n$ (**2**), and $[Gd(Hnica)(H_2O)_2SO_4]_n$ (**3**) to 2D polymers $\{[Pr_3(Hnica)_6(H_2O)_9]\cdot 3H_2O\cdot SO_4\cdot NO_3\}_n$ (**4**), $\{[Nd_3(Hnica)_6(H_2O)_9]\cdot 3H_2O\cdot SO_4\cdot NO_3\}_n$ (**5**), and $\{[Gd(Hnica)_2(H_2O)_2]\cdot ClO_4\cdot H_2O\}_n$ (**6**), respectively. All of the complexes (**1**−**6**) have been characterized by elemental analysis, IR spectra, UV−vis spectra, and X-ray single-crystal diffraction. Magnetic studies indicate ferromagnetic interactions between gadolinium(III) ions in **3** and **6** and antiferromagnetic interactions in **1**, **2**, **4**, and **5**.

Experimental Section

Materials and Characterization Techniques. All reagents and solvents employed were commercially available and used as received without further purification. Elemental analyses for C, H, and N were obtained at the Institute of Elemental Organic Chemistry, Nankai University. The FT-IR spectra were measured on a Bruker Tensor 27 Spectrometer on KBr disks. The UV−vis spectra were measured on a JASCO V-570 Spectrophotometer. Variable-temperature magnetic susceptibilities were measured on a SQUID MPMS XL-7 magnetometer. Diamagnetic corrections were made with Pascal's constants for all of the constituent atoms.

Preparations. $Pr(Hnica)(H_2O)_2SO_4]_n$ (1). A mixture of H_2nica (0.0834 g, 0.6 mmol), $Pr(NO_3)_3\cdot 6H_2O$ (0.1740 g, 0.4 mmol), $MnSO_4\cdot H_2O$ (0.0676 g, 0.4 mmol), and H_2O (12 mL) was put in a 25 mL acid digestion bomb and heated at 180 °C for 3 days. Green crystals were collected and washed with water (2 × 5 mL) and diethyl ether (2 × 5 mL). Yield: 49% (based on Pr). Anal. calcd for $C_6H_8NO_9PrS$ (411.10): C, 17.53; H, 1.96; N, 3.41. Found: C, 17.89; H, 1.59; N, 3.69. IR (KBr cm^{-1}): 3411 (br), 1632 (vs), 1555 (s), 1513 (s), 1472 (s), 1429 (m), 1390 (m), 1321 (w), 1234 (w), 1115 (s), 911 (w), 784 (w), 607 (m).

$[Nd(Hnica)(H_2O)_2SO_4]_n$ (2). Purple crystals were obtained following a procedure similar to that for **1** except that $Pr(NO_3)_3\cdot 6H_2O$ was replaced by $Nd(NO_3)_3\cdot 6H_2O$. Yield: 51% (based on Nd). Anal. calcd for $C_6H_8NNdO_9S$ (414.43): C, 17.39; H, 1.95; N, 3.38. Found: C, 17.07; H, 2.34; N, 3.57. IR (KBr, cm^{-1}): 3364 (br), 1632 (vs), 1554 (s), 1516 (s), 1473 (s), 1429 (m), 1391 (m), 1321 (w), 1234 (w), 1117 (s), 911 (w), 783 (w), 608 (m).

$[Gd(Hnica)(H_2O)_2SO_4]_n$ (3). Colorless crystals were obtained following a procedure similar to that for **1** except that $Pr(NO_3)_3\cdot 6H_2O$ was replaced by $Gd(ClO_4)_3\cdot 6H_2O$. Yield: 53% (based on Gd). Anal. calcd for $C_6H_8GdNO_9S$ (427.44): C, 16.86; H, 1.89; N, 3.28. Found: C, 16.50; H, 2.25; N, 3.32. IR (KBr, cm^{-1}): 3371 (br), 1637 (vs), 1556 (s), 1475 (m), 1430 (m), 1396 (m), 1321 (w), 1235 (m), 1123 (s), 911 (w), 784 (m), 607 (m).

$\{[Pr_3(Hnica)_6(H_2O)_9]\cdot 3H_2O\cdot SO_4\cdot NO_3\}_n$ (4). A mixture of H_2nica (0.0834 g, 0.6 mmol), $Pr(NO_3)_3\cdot 6H_2O$ (0.1740 g, 0.4 mmol), $MnSO_4\cdot H_2O$ (0.0676 g, 0.4 mmol), $(CH_3)_3CCOONa$ (0.0496 g, 0.4 mmol), and H_2O (12 mL) was put in a 25 mL acid digestion bomb and heated at 180 °C for 3 days. After a small quantity of precipitates was filtered off, green crystals were obtained by slow evaporation of the filtrate at room temperature. The product was washed with water (2 × 5 mL) and diethyl ether (2 × 5 mL). Yield: 35% (based on Pr). Anal. calcd for $C_{36}H_{48}N_7O_{37}Pr_3S$ (1625.58): C, 26.60; H, 2.98; N, 6.03. Found: C, 27.00; H, 2.63; N, 6.15. IR (KBr, cm^{-1}): 3416 (br), 1639 (vs), 1557 (s), 1462 (m), 1426 (m), 1383 (s), 1323 (w), 1234 (vw), 1113 (s), 788 (m), 571 (w).

$\{[Nd_3(Hnica)_6(H_2O)_9]\cdot 3H_2O\cdot SO_4\cdot NO_3\}_n$ (5). Purple crystals were obtained following a procedure similar to that for **4** except that $Pr(NO_3)_3\cdot 6H_2O$ was replaced by $Nd(NO_3)_3\cdot 6H_2O$. Yield: 37% (based on Nd). Anal. calcd for $C_{36}H_{48}N_7Nd_3O_{37}S$ (1635.60): C, 26.44; H, 2.96; N, 5.99. Found: C, 26.65; H, 2.60; N, 5.98. IR (KBr, cm^{-1}): 3422 (br), 1639 (vs), 1557 (s), 1462 (m), 1427 (m), 1384 (s), 1324 (w), 1235 (vw), 1113 (s), 788 (m), 571 (w).

$\{[Gd(Hnica)_2(H_2O)_2]ClO_4\cdot H_2O\}_n$ (6). Yellow crystals were obtained following a procedure similar to that for **4** except that $Pr(NO_3)_3\cdot 6H_2O$ was replaced by $Gd(ClO_4)_3\cdot 6H_2O$. Yield: 41% (based on Gd). Anal. calcd for $C_{12}H_{14}ClGdN_2O_{13}$ (586.95): C, 24.56; H, 2.40; N, 4.77. Found: C, 24.31; H, 2.67; N, 4.89. IR (KBr, cm^{-1}): 3422 (br), 1638 (vs), 1557 (s), 1474 (m), 1428 (m), 1398 (s), 1325 (w), 1238 (w), 1115 (s), 1089 (s), 777 (m), 627 (w), 578 (w).

Crystal Structure Determination. Crystals of **1**−**6** were mounted on glass fibers. Determination of the unit cell and data collection were performed with Mo Kα radiation ($\lambda = 0.71073$ Å) on a BRUKER SMART 1000 diffractometer equipped with a CCD camera. The $\omega - \varphi$ scan technique was employed. The structures were solved primarily by the direct method followed by Fourier difference techniques and were refined by the full-matrix least-squares method. The computations were performed with the SHELXL-97 program.[9,10] Non-hydrogen atoms were refined aniso-

(5) (a) Zhao, B.; Cheng, P.; Dai, Y.; Cheng, C.; Liao, D. Z.; Yan, S. P.; Jiang, Z. H.; Wang, G. L. *Angew. Chem., Int. Ed.* **2003**, *42*, 934. (b) Zhao, B.; Cheng, P.; Chen, X. Y.; Cheng, C.; Shi, W.; Liao, D. Z.; Yan, S. P.; Jiang, Z. H. *J. Am. Chem. Soc.* **2004**, *126*, 3012. (c) Zhao, B.; Chen, X. Y.; Cheng, P.; Liao, D. Z.; Yan, S. P.; Jiang, Z. H. *J. Am. Chem. Soc.* **2004**, *126*, 15394. (d) Zhao, B.; Gao, H. L.; Chen, X. Y.; Cheng, P.; Shi, W.; Liao, D. Z.; Yan, S. P.; Jiang, Z. H. *Chem.—Eur. J.* **2006**, *12*, 149.

(6) (a) Lehaire, M. L.; Scopelliti, R.; Herdeis, L.; Polborn, K.; Mayer, P.; Severin, K. *Inorg. Chem.* **2004**, *43*, 1609. (b) Brasey, T.; Scopelliti, R.; Severin, K. *Inorg. Chem.* **2005**, *44*, 160. (c) Quintal, S. M. O.; Nogueira, H. I. S.; Félix, V.; Drew, M. G. B. *Polyhedron* **2002**, *21*, 2783. (d) Yao, Y. W.; Cai, Q.; Kou, H. Z.; Li, H. D.; Wang, D.; Yu, R. B.; Chen, Y. F.; Xing, X. R. *Chem. Lett.* **2004**, *33*, 1270. (e) Chattopadhyay, S.; Fanwick, P. E.; Walton, R. A. *Inorg. Chem. Acta* **2004**, *357*, 764. (f) Yue, Y. F.; Sun, W.; Gao, E. Q.; Fang, C. J.; Xu, S.; Yan, C. H. *Inorg. Chim. Acta* **2007**, *360*, 1466. (g) Zeng, M. H.; Wu, M. C.; Zhu, L. H.; Liang, H.; Yang, X. W. *Chin. J. Chem.* **2007**, *25*, 16. (h) Wang, J. G.; Du, Q. Y.; Li, P. Y. *Jiegou Huaxue* **2006**, *25*, 747. (i) Li, Y. M.; Che, Y. X.; Zheng, J. M. *Jiegou Huaxue* **2006**, *25*, 572.

(7) (a) Soares-Santos, P.C. R.; Nogueira, H. I. S.; Rocha, J.; Félix, V.; Drew, M. G. B.; Sá Ferreira, R. A.; Carlos, L. D.; Trindade, T. *Polyhedron* **2003**, *22*, 3529. (b) Soares-Santos, P.C. R.; Almeida Paz, F. A.; Sá Ferreira, R. A.; Klinowski, J.; Carlos, L. D.; Trindade, T.; Nogueira, H. I. S. *Polyhedron* **2006**, *25*, 2471.

(8) (a) Thirumurugan, A.; Natarajan, S. *J. Mater. Chem.* **2005**, *15*, 4588. (b) Wang, C. M.; Chuang, S. T.; Chuang, Y. L.; Kao, H. M.; Lii, K. H. *J. Solid State Chem.* **2004**, *177*, 1252.

Scheme 2. The Synthesis Route for **1**−**6**

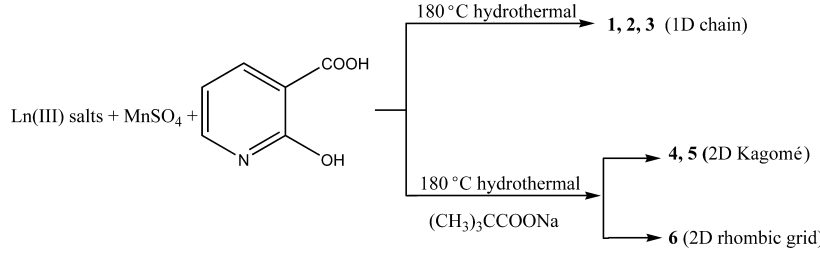

tropically, except for oxygen and nitrogen atoms of disordered uncoordinated water molecules and NO_3^- ions. The hydrogen atoms were set in calculated positions and refined as riding atoms with a common fixed isotropic thermal parameter. CCDC 681190, 681192, 652294, 681191, 681193, and 652295 contain the supplementary crystallographic data for complexes **1**−**6**, respectively. These data can be obtained free of charge *via* www.ccdc.cam.ac.uk/conts/retrieving.html (or from the Cambridge Crystallographic Data Center, 12 Union Road, Cambridge CB2 1EZ, UK; fax: (+44) 1223−336−033; or e-mail: deposit@ccdc.cam.ac.uk).

Results and Discussion

Synthesis. Coordination polymers **1**, **2**, and **3** are assembled as 1D chains in the absence of $(CH_3)_3CCOONa$. When $(CH_3)_3CCOONa$ was added to the synthetic systems of **1**, **2**, and **3**, 2D coordination polymers **4** and **5** with a Kagomé lattice and **6** with a rhombic grid were obtained (Scheme 2). This may be attributed to the template effect of $(CH_3)_3CCOONa$ and the C_3 symmetry of the $(CH_3)_3C-$ group.[11] Although pH is also an important factor in the synthesis of lanthanide coordination polymers, its effect is minor here. Comparison experiments were carried out by using a NaOH aqueous solution instead of $(CH_3)_3CCOONa$ to adjust the pH to the same values as the synthetic systems of **4**, **5**, and **6**, but **1**, **2**, and **3** were still obtained. This further confirms the template effect of the $(CH_3)_3C-$ group in the synthesis of **4**, **5**, and **6**.

Crystal Structures of 1−**6.** Single-crystal X-ray diffraction analysis revealed that **1** and **2** crystallize in monoclinic space group $P2(1)/c$, while **3** crystallizes in triclinic space group $P\bar{1}$. They all exhibit a 1D chain structure. For example, in **3**, the Gd(III) ion lies in a slightly distorted monocapped square-antiprism coordination environment (Figure 1a). O1A from hydroxyl groups; O2, O2A, O3, and O3A from carboxylic groups; O4 and O7A from SO_4^{2-} anions; and O8 and O9 from coordinated water molecules form the coordination sphere. The Gd−O bond lengths are in the range of 2.342(5)∼2.828(4) Å. The carboxylic group of $Hnica^-$ chelates one Gd(III) ion in the $\eta_{1,1}$ mode and links the other

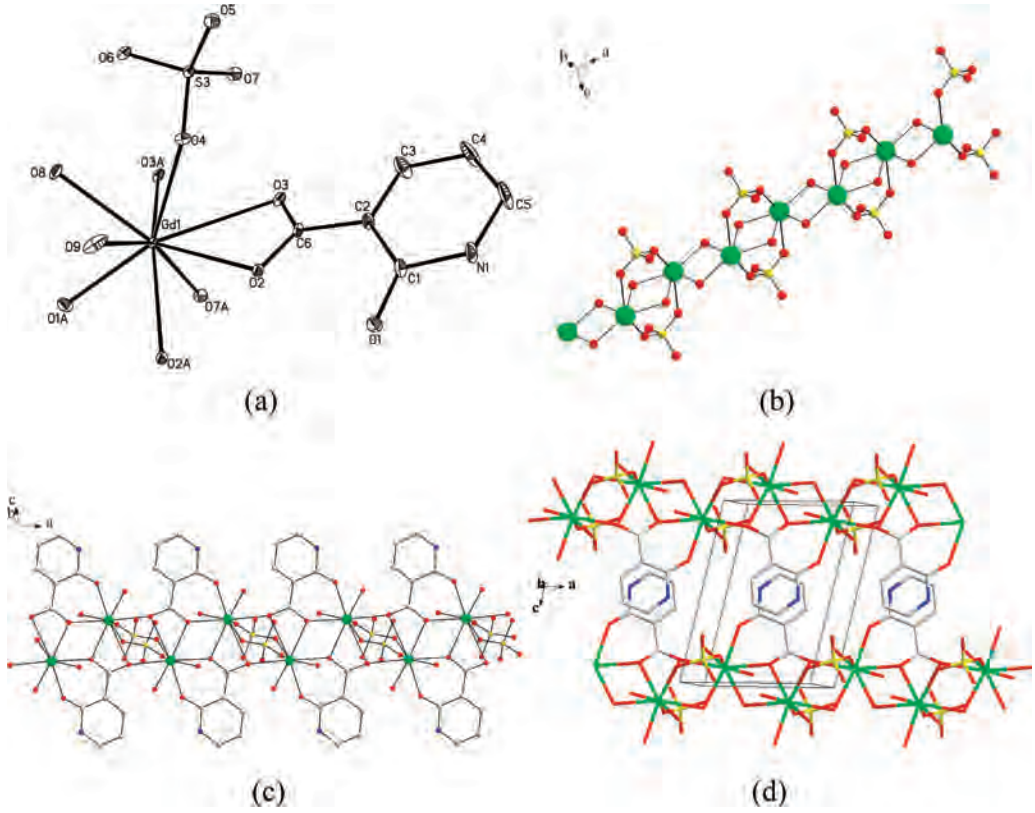

Figure 1. (a) ORTEP plot of $[Gd(Hnica)(H_2O)_2SO_4]_n$ (**3**). Thermal ellipsoids are shown at 30% probability. (b) The 1D chain of **3** bridged by SO_4^{2-}. C, N, and ketone O atoms have been omitted for clarity. (c) The 1D chain structure of **3**. (d) The packing diagram of **3**. Color code: Gd, green; O, red; N, blue; S, yellow; C, gray. All H atoms have been omitted for clarity.

Table 1. Crystal Data and Structure Refinements for **1**−**6**

	1	**2**	**3**	**4**	**5**	**6**
formula	$C_6H_8NO_9PrS$	$C_6H_8NNdO_9S$	$C_6H_8GdNO_9S$	$C_{36}H_{48}N_7O_{37}Pr_3S$	$C_{36}H_{48}N_7Nd_3O_{37}S$	$C_{12}H_{14}ClGdN_2O_{13}$
fw	411.10	414.43	427.44	1625.58	1635.60	586.95
T (K)	294(2)	294(2)	293(2)	294(2)	293(2)	294(2)
cryst syst	monoclinic	monoclinic	triclinic	trigonal	trigonal	monoclinic
space group	$P2(1)/c$	$P2(1)/c$	$P\bar{1}$	$R\bar{3}C$	$R\bar{3}C$	$P2/c$
a (Å)	7.0390(11)	6.9943(11)	6.855(11)	12.481(6)	12.6787(18)	9.898(3)
b (Å)	18.706(3)	18.637(3)	8.807(14)	12.481(6)	12.6787(18)	6.528(2)
c (Å)	8.9548(14)	8.9029(14)	9.896(17)	53.66(2)	53.746(11)	29.317(9)
α (deg)	90	90	95.22(3)	90	90	90
β (deg)	100.036(2)	99.958(2)	102.86(4)	90	90	104.029(9)
γ (deg)	90	90	102.86(4)	120	120	90
V (Å^3)	1161.0(3)	1143.1(3)	571.9(16)	7239(6)	7482(2)	1837.8(10)
Z	4	4	2	6	6	4
ρ (g/cm^3)	2.352	2.408	2.482	2.237	2.178	2.121
μ (mm^{-1})	4.416	4.765	6.021	3.151	3.241	3.828
θ (deg)	2.18−26.41	2.96−27.98	2.97−27.86	2.03−26.40	3.21−27.87	1.43−25.02
index ranges	$-8 \le h \le 4, -23 \le k \le 23, -11 \le l \le 11$	$-8 \le h \le 9, -24 \le k \le 23, -11 \le l \le 11$	$-9 \le h \le 8, -11 \le k \le 11, -13 \le l \le 12$	$-15 \le h \le 15, -15 \le k \le 12, -58 \le l \le 66$	$-14 \le h \le 13, -16 \le k \le 16, -22 \le l \le 70$	$-11 \le h \le 7, -6 \le k \le 7, -34 \le l \le 34$
reflns collected	6414	10497	6350	12790	10437	8509
ind. reflns	2372, $R_{int} = 0.0410$	2746, $R_{int} = 0.0359$	2659, $R_{int} = 0.0539$	1647, $R_{int} = 0.0471$	1978, $R_{int} = 0.0319$	3185, $R_{int} = 0.0619$
data/restraints/ parameters	2372/6/179	2746/6/164	2659/5/169	1647/2/131	1978/1/130	3185/0/264
GOF on F^2	1.091	1.060	1.116	1.213	1.088	1.124
R_1, ωR_2 [$I > 2\sigma(I)$]	0.0237, 0.0509	0.0191, 0.0486	0.0310, 0.0814	0.0491, 0.1372	0.0626, 0.1563	0.0813, 0.1984
R_1, ωR_2 (all data)	0.0299, 0.0528	0.0218, 0.0492	0.0321, 0.0819	0.0546, 0.1413	0.0632, 0.1568	0.0988, 0.2115

two adjacent Gd(III) ions. Every O atom from the carboxylic groups of Hnica$^-$ coordinates to two neighboring Gd(III) ions in the $\mu_{1,1}$ mode. In the meantime, every Gd(III) ion is linked to its neighboring Gd(III) ions by two monatomic oxygen bridges from the carboxylic groups. The angles of the oxygen bridge (Gd−O−Gd) are 117.5(1) and 109.2(1)°, and the distance between the adjacent Gds are 4.233(9) and 4.278(6) Å. SO_4^{2-} groups alternately link two adjacent Gd(III) ions in the $\mu_{1,3}$ mode (Figure 1b). Thus, carboxylic groups of Hnica$^-$ and sulfate groups both bridge the Gd(III) ions forming an infinite chain, which results in an organic−inorganic hybrid coordination polymer (Figure 1c). See Table 1 for crystal data and structure refinements for **1**−**6** and Table 2 for selected bond lengths (Å) and angles (deg) for **1**−**6**.

Complexes **4** and **5** crystallize in trigonal space group $R\bar{3}C$ and exhibit similar 2D layer structures. Here, only the structure of **4** is described in detail. As shown in Figure 2a, the Pr(III) ion lies in a slightly distorted monocapped square-antiprism coordination geometry. O3 and O3A from hydroxyl groups; O1, O1A, O2B, and O2C from the carboxylic groups; and O4, O4A, and O5 (half-occupied) from coordinated water molecules complete the coordination sphere. The Pr−O bond lengths are in the range of 2.391(6)∼2.668(2) Å. The Pr(III) ions are linked by $\mu_{1,3}$-COO bridges of the carboxylic groups of Hnica$^-$ and form adjacent hexagonal and trigonal metallic rings. Furthermore, the Pr_6 and Pr_3 rings share their edges, forming interesting Kagomé 2D lattices, as shown in Figure 2b. In a Pr_6 ring, the edge defined by the Pr···Pr distance is 6.258-Å-long, and the effective diameter is 12.481 Å. The large comby pores are filled with the free NO_3^- and SO_4^{2-} groups (Figure 2c). The observation of the Kagomé lattice is rare in lanthanide coordination polymers.

Complex **6** crystallizes in monoclinic space group $P2/c$ and exhibits a 2D lamella structure. There are two kinds of crystallographically independent Gd(III) ions. Both of them lie in a slightly distorted square-antiprism coordination environment (Figure 3a). Out of the eight oxygen atoms in the coordination sphere of Gd1, four are provided by carboxylic groups in the monodentate mode (O2, O2A, O4, and O4A), and the others are from four coordinated water molecules (O7, O7A, O8, and O8A). For Gd2, O3, O3B, O6B, and O6C from hydroxyl groups, O1, O1B, O5B, and O5C from the carboxylic groups make the coordination sphere. The Gd−O bond lengths are in the range of 2.329(12)∼2.495(12) Å. Gd1 and Gd2 are linked by $\mu_{1,3}$ carboxylic groups in an alternating way, which results in a 2D layer structure composed of rhombic grids with dimensions of 5.903 Å × 5.945 Å (Figure 3b,c). The 2D layers further overlap in a slipped fashion with the nearest Gd···Gd separation of 14.320(4) Å in the adjacent layers (Figure 3d).

In **1**−**6**, the bond lengths of C···O and N···C of the pyridine rings are in the range of 1.23(1)∼1.27(2) and 1.34 (1)∼1.39(2) Å, respectively. The bond length of C···O is shorter than that of C−O (H) (1.41−1.44 Å), which suggests that the Hnica$^-$ is exhibited as a pyridone form. This result is in accord with the conclusion that polar solvents strongly favor the pyridone form.[12]

IR and UV−Vis Spectra. The FT-IR spectra of **1**−**6** all show strong broad bands (2700−3700 cm^{-1}) of $\nu(H_2O)$, but the central positions of the bands are different (3411 cm^{-1} for **1**, 3364 cm^{-1} for **2**, 3371 cm^{-1} for **3**, 3416 cm^{-1} for **4**, 3422 cm^{-1} for **5**, and 3422 cm^{-1} for **6**). The spectra of **1**−**3** are similar because they have the same backbones. For example, in **1**, the strong peak at 1632 cm^{-1} is attributed to the antisymmetry stretching of the carboxylic groups, and the symmetrical stretch appears at 1472 cm^{-1}. The difference between ν_{as} and ν_s is 160 cm^{-1}, which is smaller than 200 cm^{-1}. This indicates the chelating mode of the carboxylic groups,[13] which is in accord with the X-ray crystal analysis. The spectra of **4** and **5** are also similar. In **4**, the ν_{as} of the carboxylic groups is shifted to a higher frequency at 1639 cm^{-1} compared to **1**, and the ν_s of the carboxylic groups appears at 1383 cm^{-1}. For **6**, the ν_{as} and ν_s of the carboxylic groups appear at 1638 and 1398 cm^{-1}, respectively. The peaks at 1088 and 627 cm^{-1} are due to the ClO_4^- anion.[13]

Table 2. Selected Bond Lengths (Å) and Angles (deg) for **1**−**6**[a]

		Complex **1**			
Pr(1)−O(1)	2.391(2)	Pr(1)−O(2)#3	2.525(2)	Pr(1)−O(5)	2.549(3)
Pr(1)−O(8)#1	2.417(3)	Pr(1)−O(6)	2.475(2)	Pr(1)−O(2)	2.573(2)
Pr(1)−O(4)	2.451(3)	Pr(1)−O(3)#2	2.507(2)	Pr(1)−O(3)#3	2.886(2)
O(4)−Pr(1)−O(6)	73.52(10)	O(4)−Pr(1)−O(5)	71.20(9)	O(4)−Pr(1)−O(2)	69.08(9)
O(8)#1−Pr(1)−O(3)#2	74.61(8)	O(6)−Pr(1)−O(5)	72.23(8)	O(2)#3−Pr(1)−O(2)	62.98(9)
O(6)−Pr(1)−O(3)#2	79.04(8)	O(3)#2−Pr(1)−O(5)	69.89(8)	O(8)#1−Pr(1)−O(3)#3	69.63(8)
O(6)−Pr(1)−O(2)#3	78.44(8)	O(1)−Pr(1)−O(2)	67.11(8)	O(6)−Pr(1)−O(3)#3	62.90(7)
O(1)−Pr(1)−O(5)	74.25(9)	O(8)#1−Pr(1)−O(2)	78.15(8)	O(3)#2−Pr(1)−O(3)#3	74.04(8)
		Complex **2**			
Nd(1)−O(1)	2.3731(18)	Nd(1)−O(2)#3	2.5033(18)	Nd(1)−O(5)	2.5205(18)
Nd(1)−O(8)#1	2.4023(18)	Nd(1)−O(6)	2.4601(18)	Nd(1)−O(2)	2.5497(19)
Nd(1)−O(4)	2.4312(18)	Nd(1)−O(3)#2	2.4840(17)	Nd(1)−O(3)#3	2.8662(18)
O(4)−Nd(1)−O(6)	73.59(6)	O(4)−Nd(1)−O(5)	71.23(6)	O(4)−Nd(1)−O(2)	69.24(6)
O(8)−Nd(1)−O(3)#2	74.80(6)	O(6)−Nd(1)−O(5)	72.41(6)	O(2)#3−Nd(1)−O(2)	62.91(7)
O(6)−Nd(1)−O(3)#2	79.04(6)	O(3)#2−Nd(1)−O(5)	69.72(5)	O(8)#1−Nd(1)−O(3)#3	69.65(6)
O(6)−Nd(1)−O(2)#3	78.10(6)	O(1)−Nd(1)−O(2)	67.65(6)	O(6)−Nd(1)−O(3)#3	63.00(6)
O(1)−Nd(1)−O(5)	74.03(6)	O(8)#1−Nd(1)−O(2)	77.83(6)	O(3)#2−Nd(1)−O(3)#3	73.54(6)
		Complex **3**			
Gd(1)−O(1)#1	2.340(5)	Gd(1)−O(4)	2.395(4)	Gd(1)−O(8)	2.479(4)
Gd(1)−O(7)#2	2.346(5)	Gd(1)−O(3)#2	2.409(5)	Gd(1)−O(2)#1	2.492(5)
Gd(1)−O(9)	2.374(4)	Gd(1)−O(2)	2.459(4)	Gd(1)−O(3)	2.830(5)
O(9)−Gd(1)−O(4)	73.98(14)	O(4)−Gd(1)−O(8)	72.94(14)	O(2)−Gd(1)−O(2)#1	62.51(14)
O(7)#2−Gd(1)−O(3)#2	73.55(11)	O(3)#2−Gd(1)−O(8)	68.27(13)	O(7)#2−Gd(1)−O(3)	70.28(14)
O(4)−Gd(1)−O(3)#2	78.24(12)	O(1)#1−Gd(1)−O(2)#1	69.81(11)	O(4)−Gd(1)−O(3)	62.45(15)
O(4)−Gd(1)−O(2)	76.75(16)	O(7)#2−Gd(1)−O(2)#1	78.31(11)	O(3)#2−Gd(1)−O(3)	70.78(12)
O(1)#1−Gd(1)−O(8)	71.95(13)	O(9)−Gd(1)−O(2)#1	70.88(14)	O(2)−Gd(1)−O(3)	48.23(13)
Gd(1)−O(2)−Gd(1)#1	117.5(1)	Gd(1)−O(3)−Gd(1)#2	109.2(1)		
		Complex **4**			
Pr(1)−O(3)	2.393(6)	Pr(1)−O(4)	2.458(6)	Pr(1)−O(5)	2.682(14)
Pr(1)−O(2)#2	2.410(6)	Pr(1)−O(1)	2.481(6)		
O(3)−Pr(1)−O(2)#3	78.0(2)	O(3)−Pr(1)−O(1)	66.48(19)	O(2)#2−Pr(1)−O(5)	64.70(17)
O(3)#1−Pr(1)−O(4)	67.45(19)	O(2)#3−Pr(1)−O(1)	72.5(2)	O(4)−Pr(1)−O(5)	66.00(15)
O(2)#3−Pr(1)−O(4)	71.6(2)	O(2)#2−Pr(1)−O(1)#1	72.5(2)		
		Complex **5**			
Nd(1)−O(3)	2.431(5)	Nd(1)−O(4)	2.479(5)	Nd(1)−O(5)	2.776(15)
Nd(1)−O(2)#2	2.442(5)	Nd(1)−O(1)	2.501(4)		
O(3)−Nd(1)−O(2)#3	78.51(18)	O(3)−Nd(1)−O(1)	67.62(17)	O(2)#2−Nd(1)−O(5)	62.62(15)
O(3)#1−Nd(1)−O(4)	67.41(18)	O(2)#3−Nd(1)−O(1)	73.6(2)	O(4)−Nd(1)−O(5)	65.26(13)
O(2)#3−Nd(1)−O(4)	71.83(17)				
		Complex **6**			
Gd(1)−O(4)	2.329(12)	Gd(1)−O(7)	2.495(12)	Gd(2)−O(5)#1	2.367(12)
Gd(1)−O(2)	2.335(13)	Gd(2)−O(1)	2.348(13)	Gd(2)−O(3)	2.378(13)
Gd(1)−O(8)	2.477(13)	Gd(2)−O(5)#3	2.367(12)	Gd(2)−O(6)#3	2.389(12)
O(4)−Gd(1)−O(8)	71.2(5)	O(2)−Gd(1)−O(7)	71.1(4)	O(5)#3−Gd(2)−O(6)#3	71.7(4)
O(2)−Gd(1)−O(8)	72.9(5)	O(7)−Gd(1)−O(7)#1	71.9(6)	O(5)#1−Gd(2)−O(6)#3	73.1(4)
O(8)#1−Gd(1)−O(8)	72.9(7)	O(1)−Gd(2)−O(5)#3	73.5(5)	O(3)−Gd(2)−O(6)#1	75.9(5)
O(4)−Gd(1)−O(7)	72.9(4)	O(1)−Gd(2)−O(3)	71.3(4)		

[a] For **1** and **2**: (#1) $-x, -y+1, -z+1$. (#2) $x-1, y, z$. (#3) $-x+1, -y+1, -z+1$. For **3**: (#1) $-x+1, -y+1, -z$. (#2) $-x, -y+1, -z$. For **4** and **5**: (#1) $x-y+1/3, -y+2/3, -z+1/6$. (#2) $y-2/3, x-1/3, -z+1/6$. (#3) $-x+y, -x+1, z$. For **6**: (#1) $-x+2, y, -z+1/2$. (#2) $-x+1, y, -z+1/2$. (#3) $-x+2, y+1, -z+1/2$. (#4) $x-1, y+1, z$.

The differences between ν_{as} and ν_s in **4**−**6** are all larger than that of **1**−**3**, which is in accord with the $\mu_{1,3}$-COO mode. Detailed data for all complexes are listed in the Experimental Section.

The UV−vis spectra of complexes **1**, **2**, **4**, and **5** were measured in the solid state. The spectra of **1** and **4** are similar, but the positions of the peaks are a little different. The spectrum of **1** exhibits strong peaks at *ca.* 266 and 332 nm, which are assigned to the intraligand $\pi-\pi^*$ transitions and $n-\pi^*$ transitions, respectively. The hypersensitive transition bands of the Pr(III) ion centered at *ca.* 448 and 594 nm can be assigned to the $^3H_4 \rightarrow {}^3P_2$ and $^3H_4 \rightarrow {}^1D_2$ transitions, respectively, and the band at 466 nm is due to the $^3H_4 \rightarrow {}^3P_1$ transition. The spectra of the Nd(III) complexes **2** and **5** also have small differences in the positions of the peaks. The intraligand $\pi-\pi^*$ transitions and $n-\pi^*$ transitions are observed at *ca.* 286 and 332 nm, respectively, in the spectrum of **2**. The hypersensitive transition bands are observed for Nd(III) ions at *ca.* 520 and 580 nm and can be assigned to the $^4I_{9/2} \rightarrow {}^4G_{7/2}$, $^4I_{9/2} \rightarrow {}^4G_{5/2}$, $^2G_{7/2}$ transitions, respectively, and the bands at 468, 680, and 742 nm correspond to the

(9) Sheldrick, G. M. *SHELXS 97*; University of Göttingen: Göttingen, Germany, 1997.
(10) Sheldrick, G. M. *SHELXL 97*; University of Göttingen: Göttingen, Germany, 1997.
(11) Gimeno, N.; Vilar, R. *Coord. Chem. Rev.* **2006**, *250*, 3161.
(12) Rawson, J. M.; Winpenny, R. E. P. *Coord. Chem. Rev.* **1995**, *139*, 313.
(13) Nakamoto, K. *Infrared and Raman spectra of inorganic and coordination compounds*, 4th ed.; Wiley Press: New York, 1986.

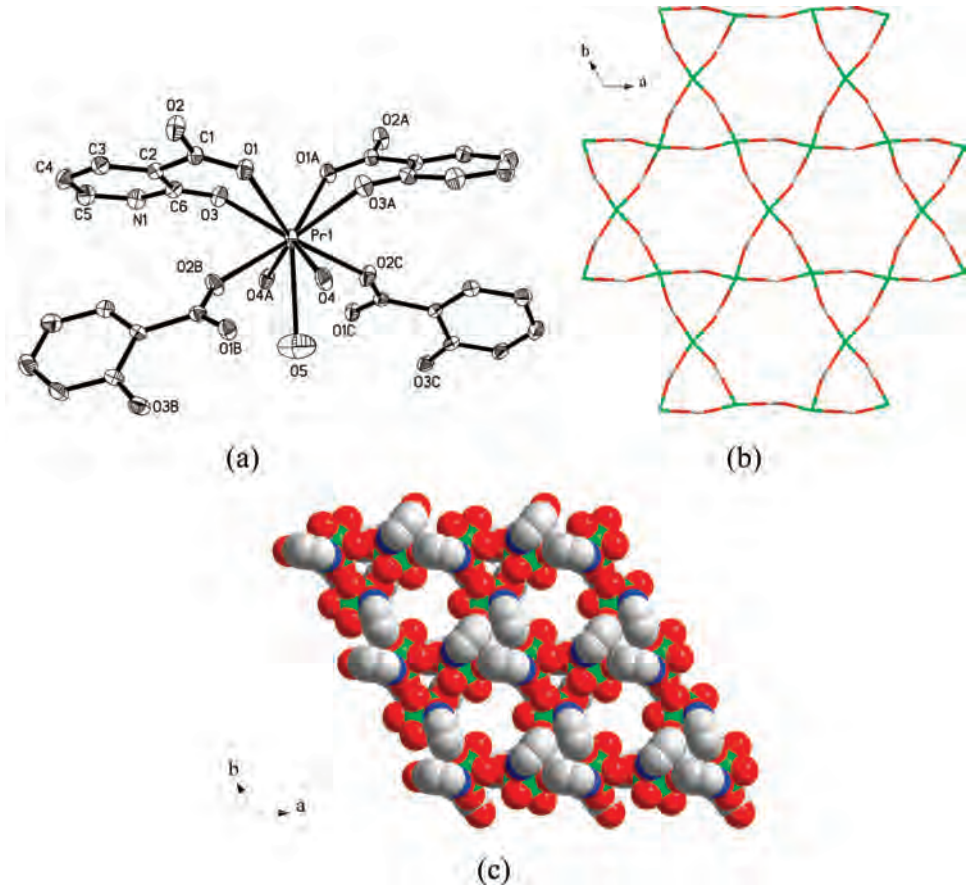

Figure 2. (a) ORTEP plot of $\{[Pr_3(Hnica)_6(H_2O)_9]\cdot 3H_2O\cdot SO_4\cdot NO_3\}_n$ (**4**). Thermal ellipsoids are shown at 30% probability. (b) 2D Kagomé lattice structure exhibited of **4**. 2-Pyridone ring atoms have been omitted for clarity. (c) Space-filling representation of Kagomé lattice in **4**. Color code: Pr, green; O, red; N, blue; C, gray. All H atoms, guest H_2O molecules, and uncoordinated SO_4^{2-} and NO_3^- ions have been omitted for clarity.

$^4I_{9/2} \rightarrow {}^2G_{9/2}$, $^4I_{9/2} \rightarrow {}^4F_{9/2}$, and $^4I_{9/2} \rightarrow {}^4F_{7/2}$ transitions, respectively.[14]

Magnetic Properties. The lanthanide(III) ions possess a first-order orbital angular momentum which prevents applying a spin-only Hamiltonian for quantitative investigation of the magnetic interactions in polymeric lanthanide complexes except for the Gd(III) complexes. Furthermore, the nature of the magnetic interactions between lanthanide(III) ions is still unclear because the inner 4f orbitals lead to weak exchange interactions, which is still an area of research interest for magneto chemists.[15]

Magnetic Properties for 1, 2, 4, and 5. The temperature dependence of magnetic susceptibilities for these four complexes is studied and shown in Figure 4. The $\chi_M T$ of **1**, **2**, **4**, and **5** at 300 K are 1.41, 1.53, 1.56, and 1.59 cm^3 K mol^{-1}, respectively. All of the values are slightly lower than the expected 1.60 and 1.63 cm^3 K mol^{-1} for one free Pr(III) ($^3H_4$, $g = 4/5$) and Nd(III) ions ($^4I_{9/2}$, $g = 8/11$) in the ground state, respectively.

Lowering the temperature caused a decrease in $\chi_M T$, which could arise from a selective depopulation of the excited crystal field state and antiferromagnetic interaction between Ln(III) (Pr or Nd) ions. There is no available expression to determine the magnetic susceptibilities of such 1D or 2D systems with large anisotropy. To obtain a rough quantitative estimation of the magnetic interaction between Ln(III) ions, the Pr(III) [or Nd(III)] ion may be assumed to exhibit a splitting of the m_j energy levels ($\hat{H} = \Delta \hat{J}_z^2$) in an axial crystal field.[16] Thus χ_{Pr} and χ_{Nd} can be described as eqs 1 and 2, respectively.

$$\chi_{Pr} = \frac{Ng^2\beta^2}{kT}\frac{2\,e^{-\Delta/kT} + 8\,e^{-4\Delta/kT} + 18\,e^{-9\Delta/kT} + 32\,e^{-16\Delta/kT}}{1 + 2\,e^{-\Delta/kT} + 2\,e^{-4\Delta/kT} + 2\,e^{-9\Delta/kT} + 2\,e^{-16\Delta/kT}} \quad (1)$$

$$\chi_{Nd} = \frac{Ng^2\beta^2}{4kT}\frac{81\,e^{-81\Delta/4kT} + 49\,e^{-49\Delta/4kT} + 25\,e^{-25\Delta/4kT} + 9\,e^{-9\Delta/4kT} + e^{-\Delta/4kT}}{e^{-81\Delta/4kT} + e^{-49\Delta/4kT} + e^{-25\Delta/4kT} + e^{-9\Delta/4kT} + e^{-\Delta/4kT}} \quad (2)$$

$$\chi_{total} = \frac{\chi_{Ln}}{1 - (2zJ'/Ng^2\beta^2)\chi_{Ln}} \quad (3)$$

In these expressions, Δ is the zero-field splitting parameter, and the Zeeman splitting was treated isotropically for the sake of simplicity.[17] The zJ' parameter based on the molecular field approximation in eq 3 is introduced to simulate the magnetic interaction between the Pr(III) [or Nd(III)] ions.[18] The best fit gives $\Delta = 1.98$ cm^{-1}, $zJ' = -0.21$ cm^{-1}, $g = 0.76$, and $R = \Sigma(\chi_{obsd} - \chi'_{cacld})^2/\Sigma(\chi_{obsd})^2 = 1.80 \times 10^{-3}$ for **1** in the range of 2−300 K. For **2**, upon lowering the temperature, χ_M increases slowly to a value of 0.025 cm^3 mol^{-1} at 25 K and then rapidly increases to 0.24 cm^3 mol^{-1} at 2 K, which leads to unsuitable fitness for data

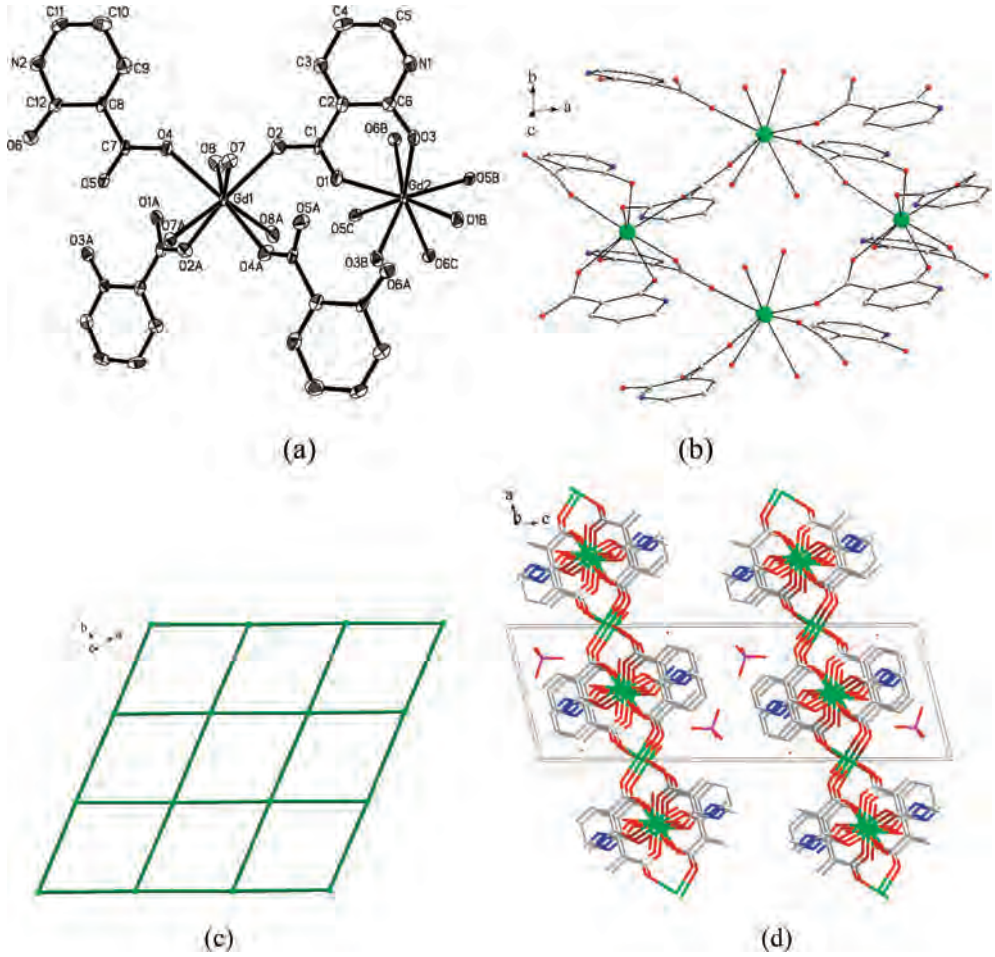

Figure 3. (a) ORTEP plot of $\{[Gd(Hnica)_2(H_2O)_2]ClO_4 \cdot H_2O\}_n$ (**6**). Uncoordinated H_2O molecules and ClO_4^- ions have been omitted for clarity. Thermal ellipsoids are shown at 30% probability. (b) Rhombic grid structure of **6**. (c) A schematic representation of the 2D rhombic grid. Nodes: Gd(III) ions. Thick lines: COO^- groups. (d) The packing diagram of **6**. Color code: Gd, green; O, red; N, blue; Cl, purple; C, gray. All H atoms have been omitted for clarity.

below 25 K. The best fit gives $\Delta = 2.00$ cm^{-1}, $zJ' = -0.4$ cm^{-1}, $g = 0.74$, and $R = 1.56 \times 10^{-3}$ in the range of 25−300 K. For **4**, the parameters are $\Delta = 4.20$ cm^{-1}, $zJ' = -0.10$ cm^{-1}, $g = 0.82$, and $R = 1.80 \times 10^{-4}$ in the range of 13−300 K. And for **5**, they are $\Delta = 2.10$ cm^{-1}, $zJ' = -0.75$ cm^{-1}, $g = 0.75$, $R = 3.06 \times 10^{-3}$ in the range of 30−300 K (Figure 4). The negative zJ' values are indicative of the antiferromagnetic interaction between the Ln(III) ions in these complexes.

Magnetic Properties for 3 and 6. The temperature dependence of magnetic susceptibilities for **3** and **6** were studied and are shown in Figure 5. The values of $\chi_M T$ of **3** and **6** at 300 K are 8.12 and 8.19 cm^3 K mol^{-1}, respectively, which are slightly higher than the expected 7.88 cm^3 K mol^{-1} per free Gd(III) ion in the $^8S_{7/2}$ ground state with an isotropic g value of 2.00. For **3**, $\chi_M T$ increases slowly with a decrease in temperature to *ca.* 30 K. When the temperature is lowered below 30 K, $\chi_M T$ increases rapidly and reaches the maximum of 9.72 cm^3 K mol^{-1} at 2 K (Figure 5a). In the case of **6**, $\chi_M T$ is almost constant in the range of 30−300 K. Further decreasing the temperature leads to an increase of $\chi_M T$. When the temperature is decreased to 2 K, $\chi_M T$ increases to 8.83 cm^3 K mol^{-1} (Figure 5b).

Taking into account that the 1D chain and 2D layer structures are composed of Gd(III) ions with a large spin value of $S = 7/2$, the expressions derived by Fisher[19] (eq 4) and Curély[20] (eq 5) were applied for **3** and **6**, respectively.

$$\chi_{1D} = \frac{Ng^2\beta^2}{3kT}\frac{S(S+1)(1+u)}{1-u} \quad (4)$$

$$\chi_{2D} = \frac{Ng^2\beta^2}{3kT}\frac{S(S+1)(W_1+W_2)}{(1-u^2)^2} \quad (5)$$

In the expressions, $u = \coth[JS(S+1)/kT] - kT/JS(S+1)$, $W_1 = (1+u^2)^2 + 4u^2$, $W_2 = 4u(1+u^2)$, J is the exchange coupling parameter between adjacent spins, and all of the other parameters have their usual meanings. For **3**, the best

(14) (a) Henric, D. E.; Fellows, R. L.; Choppin, G. R. *Coord. Chem. Rev.* **1976**, *18*, 199. (b) Baker, A. T.; Hamer, A. M.; Livingstore, S. E. *Trans. Met. Chem.* **1984**, *9*, 423.
(15) (a) Kahn, O. *Molecular Magnetism*; VCH: Weinheim, Germany, 1993. (b) Estrader, M.; Ribas, J.; Tangoulis, V.; Solans, X.; Font-Bardia, M.; Maestro, M.; Diaz, C. *Inorg. Chem.* **2006**, *45*, 8239.
(16) (a) Kahwa, I. A.; Selbin, J.; O'Connor, C. J.; Foise, J. W.; McPherson, G. L. *Inorg. Chim. Acta* **1988**, *148*, 265. (b) Tang, J. K.; Wang, Q. L.; Si-Shu, F.; Liao, D. Z.; Jiang, Z. H.; Yan, S. P.; Cheng, P. *Inorg. Chim. Acta* **2005**, *358*, 325. (c) Li, B.; Gu, W.; Zhang, L. Z.; Qu, J.; Ma, Z. P.; Liu, X.; Liao, D. Z. *Inorg. Chem.* **2006**, *45*, 10425. (d) Ouyang, Y.; Zhang, W.; Xu, N.; Xu, G. F.; Liao, D. Z.; Yoshimura, K.; Yan, S. P.; Cheng, P. *Inorg. Chem.* **2007**, *46*, 8454.
(17) Aromi, G.; Knapp, M. J.; Claude, J. P.; Huffman, J. C.; Hendrickson, D. N.; Christou, G. *J. Am. Chem. Soc.* **1999**, *121*, 5489.
(18) O'Connor, C. J. *Prog. Inorg. Chem.* **1982**, *29*, 203.

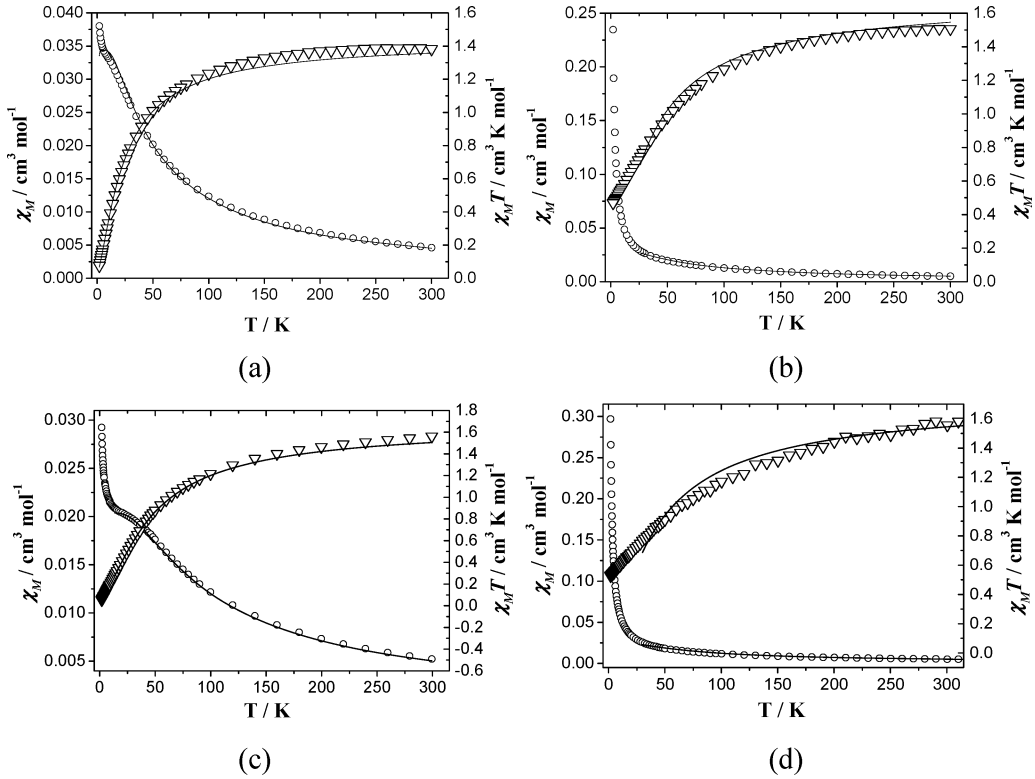

Figure 4. Temperature dependence of χ_M (○) and $\chi_M T$ (▽) for **1** (a), **2** (b), **4** (c), and **5** (d) at 0.2 T. The solid lines represent the theoretical values based on the corresponding equations.

Scheme 3. (a) Gd(III) Ions Linked in Asymmetrically Carboxylate-Bridged Mode in **3** and (b) Gd(III) Ions Linked by a COO Carboxylate Bridge, Forming a Four-Member Metal Ring in **6**

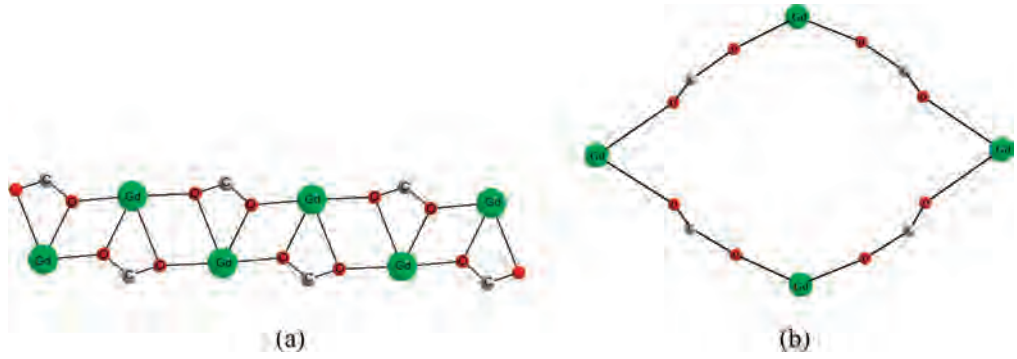

least-squares fit parameters are $g = 2.00$, $J = +0.03$ cm^{-1}, and $R = 1.23 \times 10^{-3}$. For **6**, the parameters are $g = 2.02$, $J = +0.006$ cm^{-1}, and $R = 1.39 \times 10^{-4}$. The magnitude of J is small but is on the same order as other Gd(III) complexes.[21] These results indicate ferromagnetic interactions in **3** and **6**. Magnetization curves of **3** and **6** at 2.0 K (inset of Figure 5) show that the experimental values are slightly larger than the calculated values in the low-field region, which supports the occurrence of ferromagnetic interaction.[21c]

Different bridging modes may result in different magnitudes of ferromagnetic interaction. Ferromagnetic interaction occurs in **3** when Gd(III) ions are linked by monatomic bridges with Gd−O−Gd angles of 117.5(1) and 109.2(1)° (Scheme 3a). The ferromagnetic interaction in **6** (Scheme 3b) is more interesting, though weaker than that of **3** since ferromagnetic interaction was never found in the Gd(III) complexes only bridged by $\mu_{1,3}$-COO groups. Reports on ferromagnetic coupling between Gd(III) ions are limited,[21] and what governs the nature is still unknown. In this work, the ferromagnetic interaction may be due to the accidental orthogonality between the magnetic orbitals of the interacting Gd(III) ions with suitable bridging angles and Gd···Gd distances.[21e−g] On the other hand, ab initio computations applied to Gd(III) complexes suggest that the origin of the ferromagnetic interaction of the two Gd(III) ions may also come from the spin polarization effect through the monatomic oxygen and COO carboxylate bridges.[22] The origin of the ferromagnetic interaction between Gd(III) ions needs to be further explored in the future.

(19) Fisher, M. E. *Am. J. Phys.* **1964**, *32*, 343.
(20) (a) Curély, J. *Europhys. Lett.* **1995**, *32*, 529. (b) Curély, J. *Physica B* **1998**, *245*, 263. (c) Delgado, F. S.; Kerbellec, N.; Ruiz-Pérez, C.; Cano, J.; Lloret, F.; Julve, M. *Inorg. Chem.* **2006**, *45*, 1012.

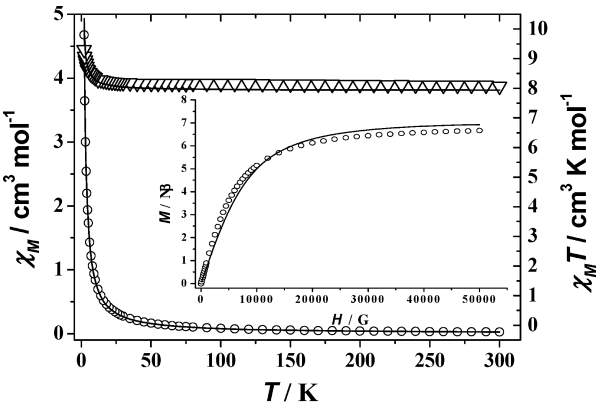

(a)

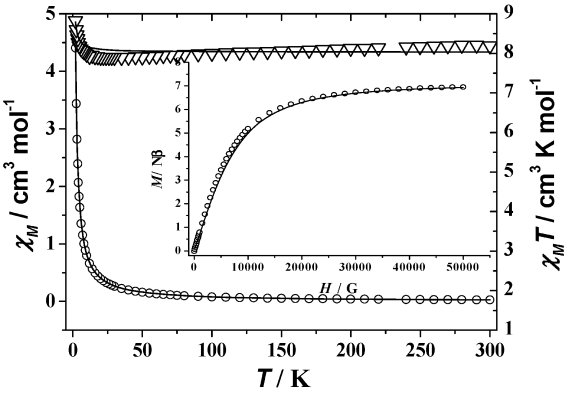

(b)

Figure 5. Temperature dependence of χ_M (○) and $\chi_M T$ (▽) for **3** (a) and **6** (b) at 0.1 T. The solid lines represent the theoretical values based on the corresponding equations. Inset: magnetic-field dependence of the molar magnetization (○) of **3** and **6** observed at 2.0 K. The solid line is the Brillouin function for the magnetically isolated Gd(III) ion with $g = 2.0$.

Conclusion

In summary, by using multidentate ligand 2-hydroxynicotinic acid, six lanthanide coordination polymers have been synthesized under hydrothermal conditions. Adding the template agent $(CH_3)_3CCOONa$ transforms the structures from 1D Ln−O−Ln chains (**1**, **2**, and **3**) to 2D layers (**4**, **5**, and **6**). To the best of our knowledge, **4** and **5** are the first examples of lanthanide coordination polymers exhibiting a Kagomé lattice structure, which will contribute to the crystal engineering of lanthanide compounds. Magnetic studies reveal that there are antiferromagnetic interactions between the lanthanide ions in the polymeric Pr(III) and Nd(III) complexes (**1**, **2**, **4**, and **5**) and rare ferromagnetic interactions in the polymeric Gd(III) complexes (**3** and **6**).

Acknowledgment. This work was supported by the National Natural Science Foundation of China (Nos. 20631030 and 20601014) and National Basic Research Program of China (973 Program, 2007CB815305).

Supporting Information Available: This material is available free of charge via the Internet at http://pubs.acs.org.

IC800623V

(21) (a) Costes, J.-P.; Clemente-Juan, J. M.; Dahan, F.; Nicodéme, F.; Verelst, M. *Angew. Chem., Int. Ed.* **2002**, *41*, 2–323. (b) Costes, J.-P.; Clemente-Juan, J.-M.; Dahan, F.; Nicodème, F. *Dalton Trans.* **2003**, 1272. (c) Hatscher, S. T.; Urland, W. *Angew. Chem., Int. Ed.* **2003**, *42*, 2862. (d) Hou, H. W.; Li, G.; Li, L. K.; Zhu, Y.; Meng, X. R.; Fan, Y. T. *Inorg. Chem.* **2003**, *42*, 428. (e) Hernández-Molina, M.; Ruiz-Pérez, C.; López, T.; Lloret, F.; Julve, M. *Inorg. Chem.* **2003**, *42*, 5456. (f) Baggio, R.; Calvo, R.; Garland, M. T.; Pena, O.; Perec, M.; Rizzi, A. *Inorg. Chem.* **2005**, *44*, 8979. (g) Canadillas-Delgado, L.; Pasán, J.; Fabelo, O.; Hernández-Molina, M.; Lloret, F.; Julve, M.; Ruiz-Pérez, C. *Inorg. Chem.* **2006**, *45*, 10585. (h) Manna, S. C.; Zangrando, E.; Bencini, A.; Benelli, C.; Chaudhuri, N. R. *Inorg. Chem.* **2006**, *45*, 9114. (i) Rohde, A.; Hatscher, S. T.; Urland, W. *J. Alloys Compd.* **2004**, *374*, 137. (j) Rohde, A.; Urland, W. *J. Alloys Compd.* **2006**, *408−412*, 618. (k) Novitchi, G.; Shova, S.; Costes, J.-P.; Mamula, O.; Gdaniec, M. *Inorg. Chim. Acta* **2005**, *358*, 4437. (l) Wu, C. D. *Inorg. Chem. Commun.* **2006**, *9*, 1223.

(22) Zhu, L.; Yao, K. L.; Liu, Z. L. *Phys. Rev. B: Condens. Matter Mater. Phys.* **2007**, *76*, 134409.